Intra–cavity generation of Bessel–like beams with longitudinally dependent cone angles

Igor A. Litvin,[1,2]* Nikolai A. Khilo,[3] Andrew Forbes[1,4] and Vladimir N. Belyi[3]

[1]*CSIR National Laser Centre, PO Box 395, Pretoria 0001, South Africa*
[2]*Laser Research Institute, University of Stellenbosch, Stellenbosch 7602, South Africa*
[3]*B.I. Stepanov Institute of Physics, NASB, 68, Nezavisimosti ave., 220072 Minsk, Belarus*
[4]*School of Physics, University of KwaZulu-Natal, Private Bag X54001, Durban 4000, South Africa*
*ILitvin@csir.co.za

Abstract: We report on two resonator systems for producing Bessel–like beams with longitudinally dependent cone angles (LDBLBs). Such beams have extended propagation distances as compared to conventional Bessel–Gauss beams, with a far field pattern that is also Bessel–like in structure (i.e. not an annular ring). The first resonator system is based on a lens doublet with spherical aberration, while the second resonator system makes use of intra–cavity axicons and lens. In both cases we show that the LDBLB is the lowest loss fundamental mode of the cavity, and show theoretically the extended propagation distance expected from such beams.

©2010 Optical Society of America

OCIS codes: (140.3410) Laser resonators; (140.3295) Laser beam characterization.

References and links

1. J. Durnin, "Exact solutions for nondiffracting beams. The scalar theory," J. Opt. Soc. Am. B **4**(4), 651 (1987).
2. J. Durnin, J. J. Miceli, Jr., and J. H. Eberly, "Diffraction-free beams," Phys. Rev. Lett. **58**(15), 1499–1501 (1987).
3. A. Vasara, J. Turunen, and A. T. Friberg, "Realization of general nondiffracting beams with computer-generated holograms," J. Opt. Soc. Am. A **6**(11), 1748–1754 (1989).
4. R. M. Herman, and T. A. Wiggins, "Production and uses of diffractionless beams," J. Opt. Soc. Am. A **8**(6), 932–942 (1991).
5. Z. Jaroszewicz, Axicons: Design and Propagation Properties, Vol. 5 of Research and Development Treatise (SPIE Polish Chapter, Warsaw, 1997).
6. A. N. Khilo, E. G. Katranji, and A. A. Ryzhevich, "Axicon-based. Bessel resonator: Analytical description and experiment," J. Opt. Soc. Am. A **18**(8), 1986 (2001).
7. J. Rogel-Salazar, G. H. C. New, and S. Chavez-Cerda, "Bessel-Gauss beam optical resonator," Opt. Commun. **190**(1-6), 117–122 (2001).
8. I. A. Litvin, and A. Forbes, "Bessel–Gauss Resonator with Internal Amplitude Filter," Opt. Commun. **281**(9), 2385–2392 (2008).
9. V. N. Belyi, N. S. Kasak, and N. A. Khilo, "Properties of parametric frequency conversion with Bessel light beams," Opt. Commun. **162**(1-3), 169–176 (1999).
10. N. A. Khilo, E. S. Petrova, and A. A. Ryzhevich, "Transformation of the order of Bessel beams in uniaxial crystals," Quantum Electron. **31**(1), 85–89 (2001).
11. V. N. Belyi, N. S. Kazak, and N. A. Khilo, "Frequency conversion of Bessel light beams in nonlinear crystals," Quantum Electron. **30**(9), 753–766 (2000).
12. Z. Bouchal, J. Wagner, and M. Chlup, "Self-reconstruction of a distorted nondiffracting beam," Opt. Commun. **151**(4-6), 207–211 (1998).
13. I. A. Litvin, M. G. McLaren, and A. Forbes, "A conical wave approach to calculating Bessel-Gauss beam reconstruction after complex obstacles," Opt. Commun. **282**(6), 1078–1082 (2009).
14. N. Davidson, A. A. Friesem, and E. Hasman, "Holographic axilens: high resolution and long focal depth," Opt. Lett. **16**(7), 523–525 (1991).
15. Z. Jaroszewicz, and J. Morales, "Lens axicons: systems composed of a diverging aberrated lens and a perfect converging lens," J. Opt. Soc. Am. A **15**(9), 2383–2390 (1998).
16. C. Parigger, Y. Tang, D. H. Plemmons, and J. W. Lewis, "Spherical aberration effects in lens-axicon doublets: theoretical study," Appl. Opt. **36**(31), 8214–8221 (1997).
17. A. V. Goncharov, A. Burvall, and C. Dainty, "Systematic design of an anastigmatic lens axicon," Appl. Opt. **46**(24), 6076–6080 (2007).
18. T. Tanaka, and S. Yamamoto, "Comparison of aberration between axicon and lens," Opt. Commun. **184**(1-4), 113–118 (2000).
19. P. A. Bélanger, and C. Paré, "Optical resonators using graded-phase mirrors," Opt. Lett. **16**(14), 1057–1059 (1991).

20. C. Pare, and P. A. Belanger, "Custom Laser Resonators Using Graded-Phase Mirror," IEEE J. Quantum Electron. **28**(1), 355–362 (1992).
21. P. A. Bélanger, R. L. Lachance, and C. Paré, "Super-Gaussian output from a CO(2) laser by using a graded-phase mirror resonator," Opt. Lett. **17**(10), 739–741 (1992).
22. I. A. Litvin, and A. Forbes, "Intra-cavity flat-top beam generation," Opt. Express **17**(18), 15891–15903 (2009).
23. T. Aruga, "Generation of long-range nondiffracting narrow light beams," Appl. Opt. **36**(16), 3762–3768 (1997).
24. T. Aruga, S. W. Li, S. Y. Yoshikado, M. Takabe, and R. Li, "Nondiffracting narrow light beam with small atmospheric turbulence-influenced propagation," Appl. Opt. **38**(15), 3152–3156 (1999).
25. V. Belyi, A. Forbes, N. Kazak, N. Khilo, and P. Ropot, "Bessel–like beams with z–dependent cone angles," Opt. Express **18**(3), 1966–1973 (2010).

1. Introduction

The zero–order Bessel beam (J_0) as a mathematical construction was firstly introduced by Durnin [1]. Such beams have been produced by many different techniques, including illuminating an annular ring and transforming the field through a lens [2], a hologram [3], an axicon [4,5], and recently intra–cavity techniques [6–9] and the use of anisotropic crystals [10,11]. The use of a refractive axicon, or conical lens, provides the most efficient method for producing Bessel beams, due mainly to the higher transmittance compared to an annular slit, and because an axicon produces no higher–order diffracted beams as in the case of holographic elements.

Much of the interest in Bessel beams is connected with the nondiffracting nature of these beams as well as with the effect of self–reconstruction of the transverse profile after shadowing (see for example [12,13]). While inside the nondiffracting region the Bessel beam does not change its profile, at the boundary of this region the beam abruptly transforms into a conical field with the characteristic ring–shaped intensity distribution; we shall refer to this change as the "double–face" effect. The significant difference between the near–field and the far–field intensity pattern can be considered a characteristic feature of such beams, in contrast to Gaussian beams which preserve their profile while propagating in free space.

The double–face effect can be partially weakened by generating a Bessel beam with a very small cone angle γ, as the nondiffracting beam length is inversely proportional to γ.

There is an elegant approach to eliminate the double–face effect for Bessel beams via the generation of Bessel beams with decreasing cone angle γ during beam propagation. In so doing, if at $z \rightarrow \infty$ the limiting value of the angle $\gamma(z)$ is zero, then such beams will have the advantages of both Bessel and Gaussian beams. In what follows such beams will be referred to as longitudinal dependent Bessel–like beams (LDBLBs).

The methods of producing such LDBLBs can be divided into two classes, namely extra– and intra–cavity beam shaping. Extra–cavity (external) beam shaping can be achieved by manipulating the output beam from a laser with suitably chosen amplitude and/or phase elements. LDBLBs have been generated external to the cavity by a variety of techniques, including a combination of axicons and lens systems with spherical aberration and anastigmatic lens axicons with reflecting spherical surfaces [13–18]. There are obvious disadvantages to reshaping outside the cavity in comparison to intra–cavity design, not the least of which is the introduction of additional external losses and adjustment problems.

The second method of producing such beam intensity profiles, intra–cavity beam shaping, is based on generating a LDBLB directly as the cavity output mode.

Unfortunately such laser beams are not solutions to the eigenmode equations of laser resonators with spherical curvature mirrors, and thus cannot be achieved (at least not as a single mode) from conventional resonator designs. The key problem is how to calculate the required non–spherical curvature mirrors of the resonator in order to obtain the desired output field. Our approach is based on a combination of the so–called "reverse propagation technique" proposed by Belanger and Pare [19–22] together with known extra–cavity designs of obtaining BLBs [23–25]. We apply this approach to two proposed resonator systems. The first resonator system is based on a combination of diverging and converging lenses, but with spherical aberration [23]. The second resonator system is based on an axicon–lens doublet together with a second axicon [25]. We will show that for both resonator systems the desired

LDBLB is the fundamental mode, yet the spectral properties of the LDBLBs differ in the two approaches.

2. Resonator concept 1: intra–cavity aberrated lenses

One method of producing (extra–cavity) Bessel beams with longitudinally dependent cone angles ($\gamma = \gamma(z)$) is shown in Fig. 1(a), and is based on a telescope arrangement where one of the lenses has significant spherical aberration [23].
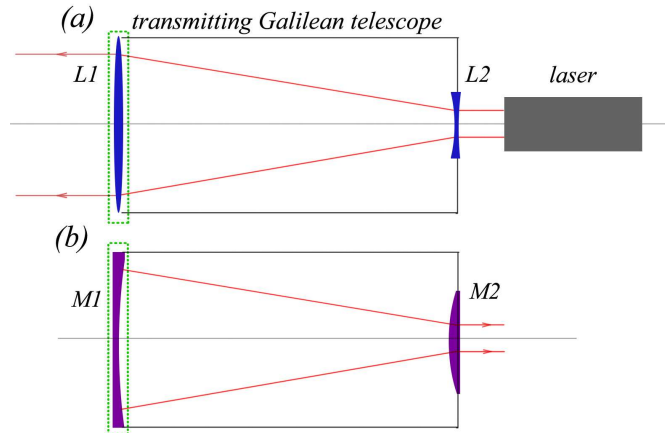

Fig. 1. (a) An extra–cavity design for producing LDBLBs by passing a Gaussian beam through a Galilean telescope system where the lenses *L2* has spherical aberration; (b) the intra–cavity resonator equivalent where *M1* has spherical aberration.

The equivalent intra–cavity design, shown in Fig. 1(b), requires two mirrors chosen such that mirror *M2* mimics lens *L2* and mirror *M1* mimics lens *L1*, but with an additional phase term to produce the conjugate field after reflection. In this case the desired field of extra–cavity system satisfies the criteria that its wavefront matches the phase of each mirror in the cavity and is the *TEM*$_{00}$ mode of the given resonator system [19–22].

In the original telescope design the optical elements were large (~10 cm in diameter) [23]. The large aperture allows raising the amount of spherical aberration easily because of this type of aberration depends strongly on the radius of the incident beam width on the lens or mirror. Obviously, the resonator system with a similar aperture is difficult to design, and one of the key problems of such a resonator system is to increase the amount of spherical aberration of the wave front of the output beam. To solve this problem we propose using a converging mirror with spherical aberration instead of a diverging lens with spherical aberration (as was proposed by Aruga [23]) [see Fig. 1(a)] and, consequently, a diverging mirror with spherical aberration in the resonator scheme [see Fig. 1(b)]. We can see from Fig. (2 (a (red)) that the beam radius on the converging mirror *M1* is almost twice the size than on the diverging one, *M2*. Therefore for the converging mirror we can use almost a 16 times weaker coefficient of the spherical aberration. Furthermore, in this case, we have to change the output mirror into a diverging mirror as well [see Fig. 1 (b)].

With these adjustments to the design, the problem is reduced to finding the shape of mirror *M1*, since the shape of mirror *M2* (as well as the resonator length) can be taken directly from the extra–cavity design. The shape of mirror *M1* must be such that after reflection the reverse propagating field should be equivalent to the phase conjugate of the field after propagation through the extra–cavity telescope system, taking into account the spherical aberration of lens *L1*. This problem can be solved analytically, as we now show. Consider the extra–cavity analogy of a Gaussian beam passing through the telescope, with the waist on *L2* with half–width w_0. Lens *L2* is a non–aberrated thin lens with focal length f_1. Lens *L1* is a converging lens of focal length *f*, together with some degree of spherical aberration (β). If the

two lenses are separated by a distance z_1, then the curvature of the wavefront at a plane just in front of *L1* may be found from the Fresnel diffraction integral:

$$a_1(\rho, z_1) = -\frac{ik_0}{2z_1} \exp\left(\frac{ik_0\rho^2}{2z_1}\right) \int_0^{R_0} \exp\left(-\frac{\rho_1^2}{w_0^2} + \frac{ik\rho_1^2}{2f_1} + \frac{ik\rho_1^2}{2z_1}\right) J_0\left(\frac{k_0\rho\rho_0}{z_1}\right) \rho_1 d\rho_1 \quad (1)$$

where $k_0 = 2\pi/\lambda$, λ is the wavelength of the light, and R_0 is the radius of the mirror. It is useful to solve Eq. (1) by applying the method of stationary phase, to give:

$$a_1(\rho, z_1) = -\frac{w_0}{w(z_1)} \exp\left[-\left(\frac{\rho}{w(z_1)}\right)^2 + \frac{ik\rho^2}{2R(z_1)} - i\alpha(z_1)\right] \quad (2)$$

where $w(z_1) = w_0\sqrt{1 + (z_1/f_1)^2 + (z_1/z_0)^2}$, $R(z_1) = z_1 \dfrac{1+(z_0/z_1)^2(1+z_1/f_1)^2}{1+(z_0/z_1f_1(1+z_1/f_1))}$,

$\alpha(z_1) = \arctan\left(\dfrac{z_1/z_0}{1+z_1/f_1}\right)$ and $z_0 = k_0 w_0^2/2$.

At the plane just after *L1* the field will be the product of a_1 and the transmission function of lens *L1* with spherical aberration, namely:

$$a_2 = a_1 \exp\left(-ik_0\rho^2/2f_2 + ik_0\beta\rho^4\right). \quad (3)$$

The transfer function for mirror *M1* is then found from [19–22]:

$$t_{M1} = a_2^*/a_2. \quad (4)$$

We simulate this resonator numerically using the well known Fox–Li approach in matrix approximation [22], with the following parameters: $\lambda = 632$ nm, $z_1 = 0.65$ m, $w_0 = 0.5$ mm, $f_1 = 0.4$ m, $f_2 = 0.7$ m, and aberration coefficient $\beta = 16 \times 10^4$ m^{-3}. The mirror radii were chosen as $R_0 = 5$ mm, corresponding to a Fresnel number of $N_f = 60$. With these parameters the phase of mirror *M1* was calculated directly from Eq. (4) and shown in Fig. 2 (a (blue)).
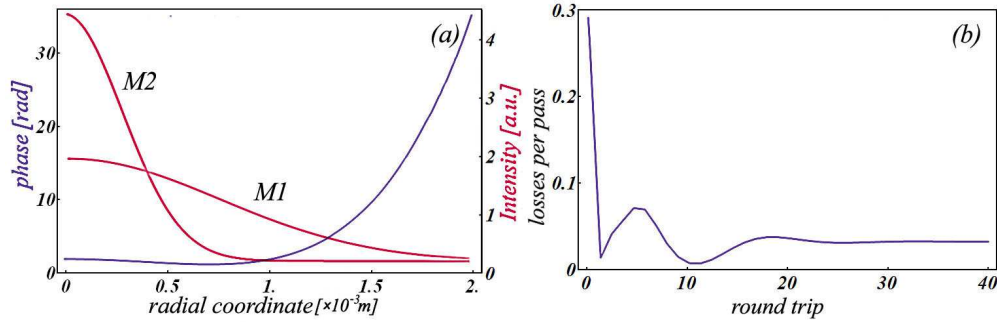

Fig. 2. The phase of mirror *M1* obtained by direct solution of Eq. (4) (a (blue)) and the intensity profiles on resonator mirror *M1* and *M2* after stabilization (a (red)). The fundamental mode stabilization as a function of the number of round trips (b).

We note from Fig. 2(b) that the fundamental mode stabilizes after only a short number of round trips; despite the relatively large Fresnel number of the system. We can understand this behaviour by considering that without any spherical aberration on mirror *M1* the resonator lies on the boundary between stable and unstable, and with the inclusion of spherical aberration the losses increase due to a shift into an unstable resonator configuration with the overall losses around 4 percent per trip.

Figure 2(a (red)) shows the intensity profiles of the beam on mirrors *M1* and *M2* after stabilization of the Fox–Li algorithm. We can see the required fields are obtained

successfully, namely Gaussian transverse intensity profile on mirror *M2* (see Eq. (1) and the field corresponding to Eq. (2) on mirror *M1*.
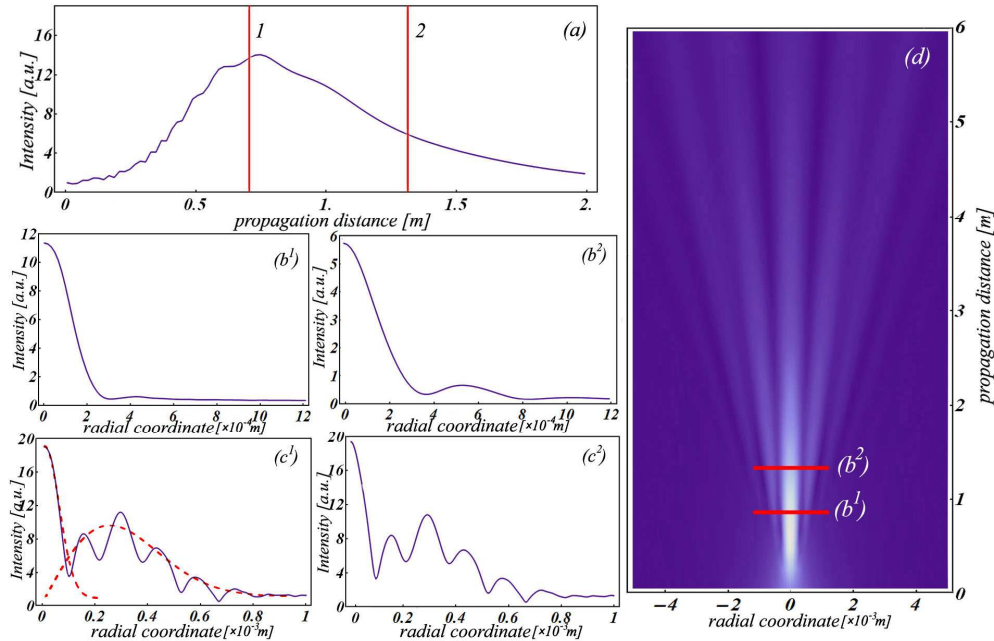

Fig. 3. The propagation properties of the output beam. (a) – longitudinal dependence of on-axial intensity, (b) – cross section of propagated beam on distance 0.7 m (1) and 1.3 m (2) correspondingly, (c) – spatial spectrum intensity view of obtained beam profiles, (d) – density plot of the propagated beam.

Figure 3(a) illustrates the change in the on-axis intensity with propagation distance z. As is seen, it is a one-peaked curve typical for Bessel beams. When z increases up to several meters or more, there occurs a slow monotonic decrease in the peak on-axis intensity with propagation distance as is typical of Gaussian beams. We also note that the field widens during propagation [see Fig. 3(b) and 3(d)], as well as picks up the ring structure of Bessel beams. Thus the output beam from the resonator has the characteristics of a Bessel–like beam outlined by others [23]. The nondiffracting properties of this beam can be noted from the spatial spectrum Fig. 3(c) which consists of two main peaks (see Fig. 3(c^1) red dashed graphs), the first central peak due to the Gaussian nature of the beam, and the second off-center peak (with some oscillations) a characteristic of the annular ring spectrum of Bessel–Gauss beams [12]. The oscillations on this annular ring are due to the composite nature of the Bessel spectrum from such Bessel–like beams, namely that the spectrum is a summation over several Bessel spectrums with close cone angles. These results are consistent with those found by the generation of such beams external to the cavity [23]. In particular, such beams have the advantages of both Gaussian and Bessel beams: long propagation distances over which the shape of the intensity does not change (Gaussian-like characteristics) and nondiffracting properties similar to Bessel beams.

3. Resonator concept 2: intra–cavity axicons

It has recently been shown that it is possible to create Bessel–like beams with longitudinally dependent cone angles, $\gamma = \gamma(z)$, by the use of axicons and lenses sans any spherical aberration [25]. This method, depicted in Fig. 4(a), consists of two axicons, *A1* and *A2*, and a thin lens *L* with focal length *F*. The Bessel beams generated by these axicons are characterized by cone angles of γ_1 and γ_2 respectively.
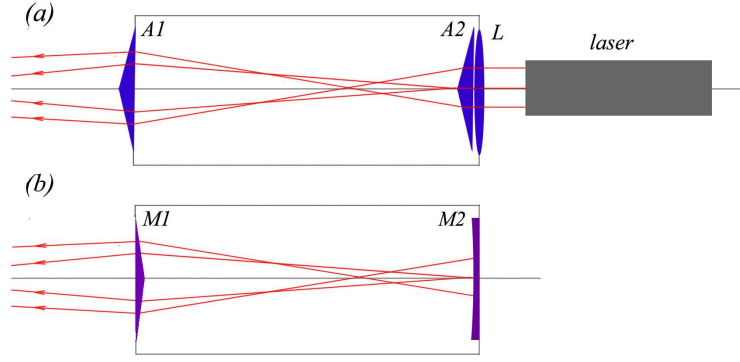
Fig. 4. (a) An extra–cavity design for producing LDBLBs by passing a doublet of axicon-lens and axicon; (b) the intra–cavity resonator equivalent.

Following the same approach as outlined in the previous section, one can construct an equivalent resonator version of this set–up, as shown in Fig. 4(b). However modelling such a system is problematic due to the fact that the apexes of the axicons are aligned with the maximum intensity of the laser beam. To solve this problem we propose using instead of a zero order Laguerre–Gaussian beam the Laguerre–Gaussian beam of first azimuthal order (m = 1, p = 0) but with a flat phase (the beam waist fits the output plane) as the initial beam to avoid maximum intensity on apexes of axicons [see Fig. 5 (a (red))].

Similarly to the first scheme, the curvature of the wave front at the output plate of the "axicons" scheme may be found from the Fresnel diffraction integral:

$$a_1(\rho, z_1) = -\frac{i}{\lambda z_1} \exp\left(\frac{ik_0 \rho^2}{2z_1}\right) \int_0^{2\pi} \int_0^{R_{a2}} \exp\left(-\frac{\rho_1^2}{\rho_0^2} - ik_0 \gamma_2 \rho_1 - \frac{ik_0 \rho \rho_1}{z_1} \cos(\phi - \phi_1)\right) \rho_1^2 \, d\rho_1 \, d\phi_1 \quad (5)$$

where $\dfrac{1}{\rho_0^2} = \dfrac{1}{w_0^2} + \dfrac{ik_0}{2F} - \dfrac{ik_0}{2z_1}$, R_{a2} – is the radius of the axicon $A2$, w_0 = 1.5 mm – the half-width of the input Laguerre-Gaussian beam.

Following the approach of the stationary phase approximation as before, we find the field at $M1$ to be given by:

$$a_1(\rho, z_1) = -\frac{i\rho F^2}{(z_1 - F)^2}\left(1 - \frac{\gamma_2 z_1}{\rho}\right)^{3/2} \exp\left[\frac{ik_0}{2z_1}\left(\rho^2 + \frac{z_1/F - 1 + iz_1/z_0}{(z_1/F - 1)^2 + (z_1/z_0)^2}(\rho - \gamma_2 z_1)^2\right)\right] \quad (6)$$

with $z_0 = k_0 w_0^2 / 2$.

At the plane just after $M1$ the field will be the product of a_1 and the transmission function of the axicon $A1$, namely:

$$a_2 = a_1 \exp\left(-ik_0 \gamma_1 \rho\right). \quad (7)$$

We simulate this resonator numerically using the well known Fox–Li approach in matrix approximation [22], with the following parameters: λ = 632 nm, z_1 = 0.65 m, w_0 = 1.5 mm, γ_1 = 0.3 degree, γ_2 = 0.1 degree, F = 0.65 z_1. The mirror radii were chosen as $R_{a1,2}$ = 5 mm, corresponding to a Fresnel number of N_f = 60. With these parameters the phase of mirror $M2$ was calculated directly from Eq. (7) and shown in Fig. 5 (a (blue)).
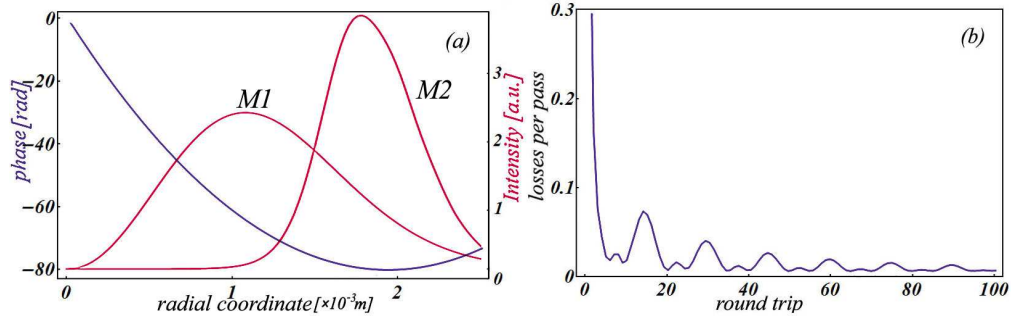
Fig. 5. The phase of mirror *M2* obtained by the direct solution of Eq. (7) (a (blue)) and the intensity profiles on resonator mirror *M2* and *M1* after stabilization (a (red)). The fundamental mode stabilization as a function of the number of round trips (b).

The stabilization process for this resonator system [Fig. 5(b)] behaves differently to that shown earlier. Firstly, the stabilization process requires more round trips for similar Fresnel numbers, and secondly, we note an oscillation in the process which may be explained by the interference of the low order modes during stabilization.

The resulting fields on both the mirrors after stabilization are shown in Fig. 5 (a (red)). The obtained transverse field distributions on both mirrors fits the required transverse field distributions of Eqs. (5), 6). The change in the on-axis intensity with propagation distance z can be seen in Fig. 6(a). It is a one-peaked curve typical for Bessel beams and with z increasing there occurs a slow monotonic decrease in the peak on-axis intensity with a propagation distance as is typical of Gaussian beams. The obtained behavior is similar to the telescope scheme [see Fig. 3(a)].

During propagation the intensity profile of the obtained beam is getting wider and the transverse intensity profile becomes close to a Bessel beam profile with a longitudinal change of the cone angle as we can see in Fig. 6(b), 6(d).

One of the major features of these beams is the dramatically increased propagation distance over which the beam intensity remains enveloped by a Bessel function. In fact, the Bessel character remains to the far field (infinity), and have been tested in the laboratory up to several tens of meters [25]. By contrast, one of the popular methods for Bessel–Gauss beam generation is employment of an axicon and a Gaussian beam [4,5]; using the same values for the Gaussian beam width, w_0, and axicon cone angle, γ_1, we find that such a Bessel–Gauss beam would have a nondiffracting length of approximately 0.3 m. Thus while the LDBLBs slowly diverge during propagation, the enveloping function remains Bessel-like. Clearly there are applications where this shape invariance during propagation would be desirable.

From the view of the spatial spectra of the obtained beam and because of the spatial spectra profile of the Bessel–Gauss beam has displacement Gauss view we can suppose that the obtained beam can be described as the sum of Bessel–Gauss beams with different and discrete differences in the cone angles [see Fig. 6 (c)]. This representation can be used for an easy explanation of the self–reconstruction properties of this class of longitudinal dependant Bessel like beams [12].

However, if the cone angle of the obtained beam changes with distance, namely the decrease of the cone angle is observed, we anticipate a decrease of the annular ring radius of the spatial spectra. Nevertheless the absolute value of the spatial spectra must be conserved [see Fig. 3(c) and 6(c)] To avoid the mismatch of the spatial spectra and the propagation properties of the obtained beam we propose the following explanation. We can describe the spatial spectrum of the obtained beam as a sum of Bessel–Gauss beams with different and discrete differences in cone angles [see Fig. 6 (c)] and the initial field has an intensity which is similar to the displaced Gaussian [see Fig. 5 (a)]. Therefore we can expect that the rays, radiating from the displaced Gauss peak and the associating with the different Bessel–Gauss beams, will intersect the central part of the beam on different distances [see the output rays on Fig. 4 (a), 4(b)]. The distance will be longer for Bessel–Gauss beams with a smaller cone

angle and vice versa which is why the central part of the beam must be described by a Bessel function with a decreasing cone angle during the propagation [see Fig. 6 (c)]. Consequently we must expect the self–reconstruction distance to increase in distance corresponding to the cone angle of the central part of the beam [12].
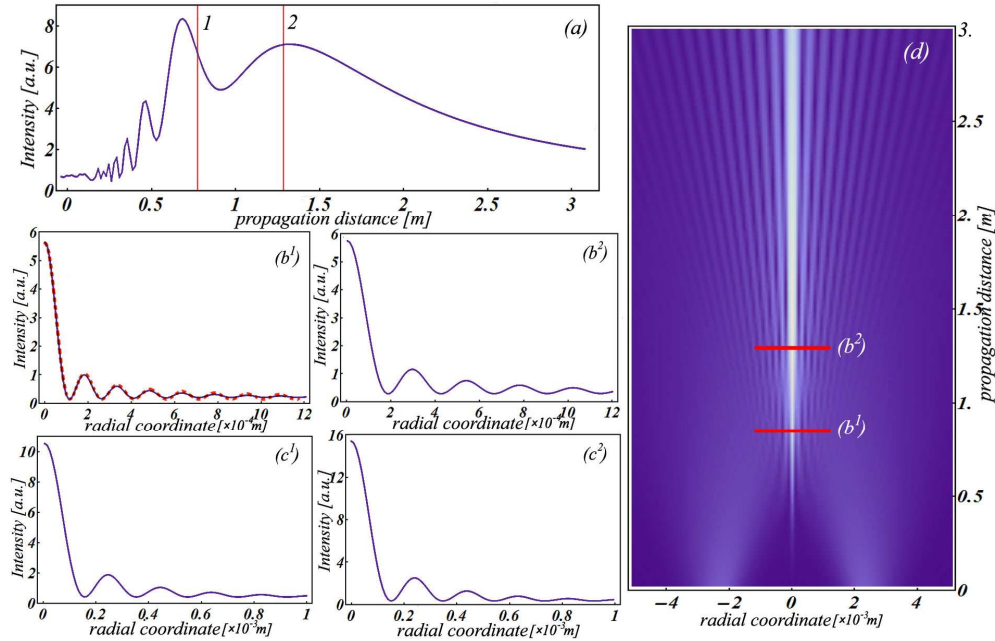

Fig. 6. The propagation properties of the output beam of the intra–cavity axicons scheme. (a) – longitudinal dependence of the central peak, (b) – cross section of the propagated beam on distance 0.7 m (1) and 1.3 m (2) correspondingly, red dotes on (b^1) – the Bessel function of 0 order with radial wave number equal to 2.05×10^4 m^{-1} (c) – spatial spectrum intensity view of the obtained beam profiles, (d) – density plot of the propagated beam.

4. Conclusion

We have outlined two resonator systems for producing longitudinally dependent Bessel–like beams as the output TEM_{00} mode. The first resonator system is based on a doublet of the diverging and converging lenses with spherical aberration [23]. The second resonator system is composed of lens-axicon doublet and a second axicon [25]. The difference in the spectrums and intensity profiles of the obtained beams leads to differences in both the propagation properties and the nondiffracting property of the resulting beams that we can see in Fig. 3 and Fig. 6. The different stabilization behavior of these systems was observed and results from the difference in the stability parameter of given cavities [see Fig. 2(b) and Fig. 5(b)]. Because of the field on one of the mirrors of both the resonator systems has the Laguerre–Gaussian view, we can employ the widely applicable methods for selection of required mode and depressing undesired ones, which are extensively used in the conventional resonators, for example the inclusion of suitable apertures. We can conclude that both resonator systems can be used for producing longitudinally dependant Bessel–like beams and obtained beams have close but different nondifraction and propagation properties (see Fig. 3, 6). The shape invariance of such beams over extended distances as compared to regular Bessel-Gauss beams may be desirable for many applications.